Nature-Inspired Flow-Fields and Water Management for PEM Fuel Cells

P. Trogadas[*a], J. I. S. Cho[†*a], V. S. Bethapudi[a,b], P. Shearing[b], D. J. L. Brett[b], and M.-O. Coppens[†a]

a. EPSRC "Frontier Engineering" Centre for Nature Inspired Engineering & Department of Chemical Engineering, University College London, London WC1E 7JE, UK.
b. Electrochemical Innovation Lab, Department of Chemical Engineering, University College London, London WC1E 7JE, UK.
* Both authors contributed equally.
† Corresponding authors: in.cho.13@alumni.ucl.ac.uk; m.coppens@ucl.ac.uk

A nature-inspired solution methodology is used to address flooding issues at high relative humidity (RH) in proton exchange membrane fuel cells (PEMFCs). The water management strategy is based on the mechanism employed by certain lizards, residing in arid environments, to drink water. A thin graphite plate with laser engraved capillaries is installed on our best performing lung-inspired flow-field based PEMFCs with 4 generations (N) and its performance at 100% RH is compared against commercial serpentine flow-field and lung-inspired flow-field ($N = 4$) based PEMFCs. Initial results demonstrated significant improvement in the performance and operating range of the lung-inspired flow-field based PEMFC when implementing this water management mechanism.

Introduction

Proton exchange membrane fuel cells (PEMFCs) are an increasingly popular energy conversion technology because they are emission-free if hydrogen from renewable sources is used. Their facile start-up, high energy density, and low operating temperature transform them into ideal candidates for portable and automotive applications. However, there are still obstacles to overcome, such as the high cost and under-utilization of the electrocatalyst, durability issues, flooding at high relative humidity, and uneven reactant distribution across the surface of the membrane electrode assembly (MEA), resulting in performance losses.(1)

Recently, we employed our systematic, nature-inspired solution methodology(2) to solve the non-uniform distribution of reactants issue in PEMFCs. Our nature-inspired approach(1, 3-6) does not copy nature, as in a bio-imitating approach, but, instead, it thoroughly investigates the relation between the function and the structure of the biological organism, considering the differences in the context of fuel cell technology and in the constraints between the biological model and the technical application.

The design of the new flow-fields is inspired by the structure and function of the human lung, which serves a similar role in nature by uniformly distributing air throughout its volume and oxygenating the blood cells. The complex architecture of the

airway tree consists of two regions: the upper region with 14-16 branching generations decreases the convection-driven gas flow from the trachea to the bronchioles and equates it to the diffusion-driven gas transport from the bronchioles to the acini, located at the lower region (7-9 generations). In addition, the diameters of successive branches obey Murray's cube scaling law. As a result, constant entropy is produced at each branching level in both regions, and, hence, there is minimal overall entropy production over the entire airway tree of the lung.(1, 3, 7)

Based on these key characteristics of the human lung, a detailed model is constructed in COMSOL to calculate the optimum number of generations required for the convection-driven flow to be equal to the diffusion-driven flow (Pé = 1).(1, 7) The ideal number of generations, N, to minimize overall entropy production in a 10 cm^2 flow-field is $N = 6$, where Pé ~ 1; for $N < 4$, gas flow is dominated by convection; whereas, for $N > 7$, gas transport is dominated by diffusion.(1, 7) These modeling results serve as the basis for the engineering of lung-inspired flow-fields with $N = 3, 4$, and 5 generations, and 10 and 25 cm^2 surface area, via stereolithography (Fig. 1). Lung-inspired flow-field based PEMFCs with $N = 4$ demonstrate ~ 25% higher current and power density than commercial serpentine flow-field based PEMFCs, but they are prone to flooding at high (100%) relative humidity (RH) due to the low pressure drop in their channels, resulting in slow gas flow, insufficient to rapidly remove the water from the cell.(8)
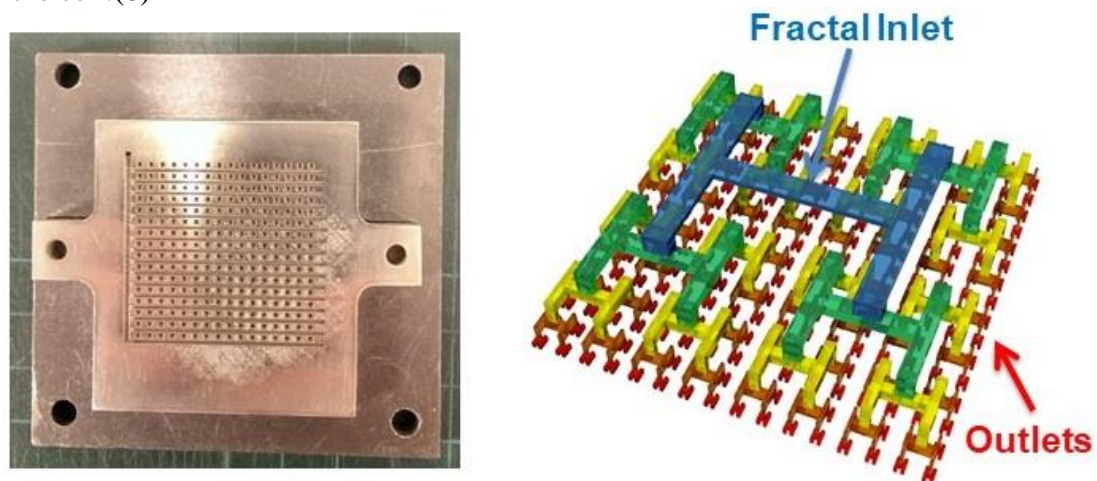

Figure 1. Engineered lung-inspired flow fields with several branching generations (green: N=2, yellow: N=3, red: N=4).

To address the flooding issues of PEMFCs at high RH, we take inspiration from lizards living in arid environments, and specifically from the mechanism they employ to drink water. Certain lizards, such as the Texan horned lizard, the Australian thorny devil, or the Arabian toad-head agama, utilize an intricate network of water harvesting channels on their back to collect water from moist ground and humidified air, then transfer it to their mouth via capillary action.(9) Based on the unique characteristics of these lizards, we employ computerized numerical control (CNC) to engineer a thin graphite plate (~ 1 mm) with a laser-engraved microchannel structure on its surface, which is then installed on our best performing lung-inspired flow-field based PEMFC with $N = 4$ generations. Its performance is evaluated against commercial serpentine and lung-inspired flow-field ($N = 4$) based PEMFCs. Initial results are presented in the following sections.

Experimental

MEA Fabrication

A 10 cm^2 MEA was fabricated *in-house* by hot pressing a Nafion 212 membrane (DuPont, USA) and ELE0070 gas diffusion electrodes (Johnson Matthey, UK) using a 12-ton thermal press (Carver, 4122CE). The membrane was used without any pre-treatment, and the MEA was pressed at 130 °C for 3 min at 400 psi. The membrane had a thickness of 50 μm, while the platinum loading was 0.4 mg$_{Pt}$ cm^{-2}.

PEMFC Components

The PEMFC contained a lung-inspired, fractal flow-field at the cathode and a commercial, single-channel serpentine flow-field at the anode. The fractal flow-field had four branching generations; a detailed description of its dimensions and manufacturing procedure are provided elsewhere.[1] The commercial, serpentine flow-field at the anode had channel width, spacing, and depth of 1 mm, 1 mm, and 0.7 mm, respectively.

The CNC technique was used to engineer a thin graphite plate (~ 1 mm) with a laser-engraved microchannel structure on its surface. X-ray tomographic measurements (SEM Zeiss EVO10, USA) revealed that these microchannels were 0.5 mm wide and 0.3 mm deep. This graphite plate was then attached to a graphite sheet (RS series, 0.16 mm thick, 150 mm × 150 mm) with laser cut holes matching the fractal inlet holes of the lung-inspired flow-field, which was finally installed on its surface. Compression alone was enough to seal these three components together.

PEMFC Operation

For the neutron imaging measurements, PEMFC was operated without heating, while hydrogen and air at a stoichiometric ratio of 1.2 and 3, respectively, were used as fuel and oxidant. The current drawn from the cell was regulated via a DC electronic load (PLZ664W4), while LabVIEW software (National Instruments) was used for data acquisition. Galvanostatic measurements were conducted by gradually changing the current density every 10 min at 0.1 A cm^{-2} intervals until the potential dropped below 0.2 V.

For PEMFC measurements, fuel cell temperature, inlet gas flow rate and relative humidity were regulated using an 850e fuel cell station (Scribner Associates, USA). The stoichiometry at the anode and cathode were kept constant at 1.2 and 3, respectively. The inlet gas relative humidity of the anode was kept the same as the cathode (100%) and the cell temperature was set to 70°C. The outlet of both the anode and cathode was at atmospheric pressure.

Neutron Imaging

Neutron radiography was conducted at the neutron imaging facility CONRAD at Helmholtz Zentrum Berlin with a flux of $2.7 \cdot 10^9$ neutrons cm^{-2} s^{-1} and a maximum field-of-view of 12 × 12 cm^2. The fuel cell was placed in through-plane orientation to the beam to visualize liquid water across the MEA. A 100 μm thick ^{6}LiF neutron

scintillator screen converted the neutron flux into visible light, which was recorded by a CCD camera (Andor DW436N-BV, 2048 x 2048 pixels).[10]

Images were taken with an exposure time of 20 s to monitor the changes in liquid water distribution during a current hold. The employed exposure time was within the range (1-25 s) typically used for neutron imaging of PEMFCs.[8]

Water Thickness Calculation

Neutron images obtained during PEMFC operation were normalized to a reference image of the dry fuel cell (Fig. 2) before operation to obtain only the attenuation corresponding to the water content in the PEMFC. The thickness of water, t_{water}, was calculated from the relative neutron transmission (I/I_o) by inverting Lambert-Beer's law[8]:

$$t_{water} = -\frac{\ln\left(\frac{I}{I_o}\right)}{\mu_{water}}$$

[1]

where I is the intensity of the beam in operation, I_o is the intensity of the beam of the dry PEMFC, t_{water} is the thickness of water, and μ_{water} is the attenuation coefficient of water equal to 3.5 cm^{-1}, based on the measurements at the CONRAD beamline.
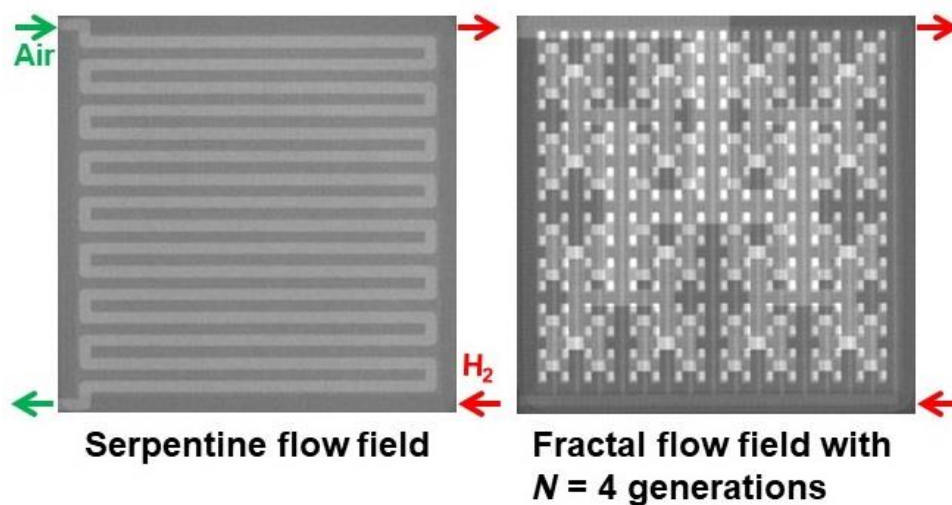

Figure 2. Radiograph of a dry cell with single serpentine flow-field, and lung-inspired flow-field ($N = 4$). Green and red arrows indicate the flow direction of air and hydrogen, respectively. In the case of a fractal flow-field, air is directed perpendicular to the plane.

Results and Discussion

The efficiency of water removal for a commercial serpentine flow-field, lung-inspired flow-field ($N = 4$), and lung-inspired flow-field ($N = 4$) with water management was accessed via neutron measurements taken during galvanostatic operation at 0.3 A cm^{-2}.

Even though the similar anode and cathode geometries of the conventional fuel cell with only serpentine flow-fields rendered it difficult to distinguish the side of the

electrode where the water was generated, differentiation was possible thanks to careful observation of droplet movement. In the anode (upper part of Fig. 3A), water droplets started to accumulate in the corners of the channels and remained stagnant during the current hold at 0.3 A cm^{-2} as a result of the slow gas flow and the absence of a large enough droplet to initiate movement across the channel. On the contrary, water droplets in the cathode (lower part of Fig. 3A) spread across the surface of the channel in the direction of the flow.

For lung-inspired flow-fields (Fig. 3B), water droplets appeared on the channel wall and merged with neighboring droplets to form slugs, which eventually blocked the channels and flooded the cell. Thus, the slow gas flow in lung-inspired flow-fields in comparison to commercial serpentine flow-fields made them susceptible to flooding, even at low current densities.

However, once the water management strategy was implemented in lung-inspired flow-fields (Fig. 3C), it was clearly visible that water accumulation occurred only on the anode side (i.e. serpentine flow-field) of lung-inspired flow-field based PEMFC; whereas, on the cathode side, the installed capillaries rapidly removed the generated water from the channels.
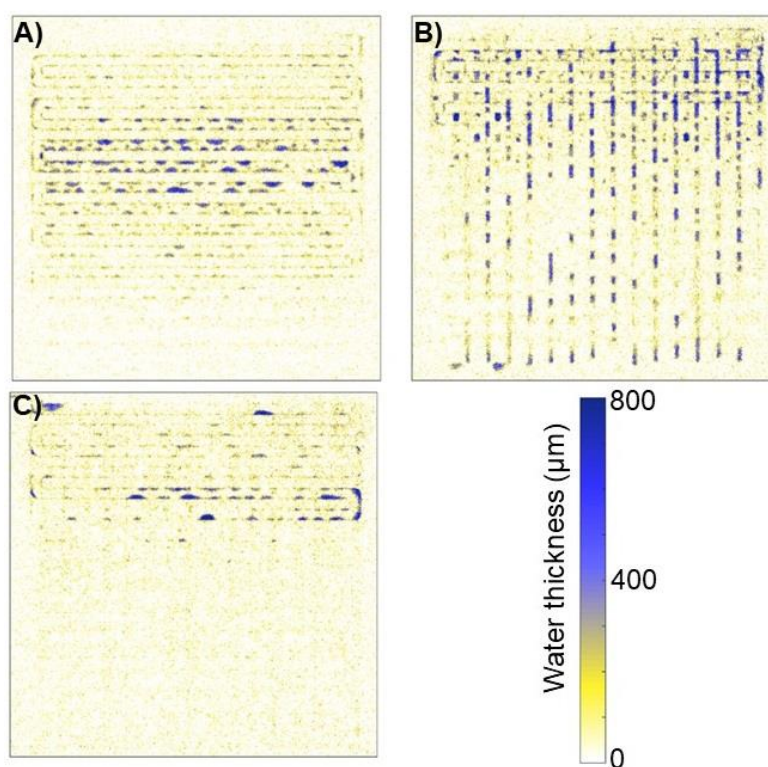

Figure 3. Neutron images showing water distribution across the commercial serpentine (A), lung-inspired with $N = 4$ (B), and lung-inspired with $N = 4$ and a water management strategy implemented (C) flow-field based PEMFCs during galvanostatic operation at 0.3 A cm^{-2} (10 cm^2 flow-field area).

The fuel cell performance of these three different flow-field designs was evaluated at 100% RH (Fig. 4). Initial results demonstrated significant improvement in fuel cell efficiency and operating range thanks to the implementation of this water management strategy in lung-inspired flow-field based PEMFCs. Commercial serpentine and lung-

inspired flow-field based PEMFCs exhibited a maximum current and power density of ~ 1.5 A cm^{-2} and ~ 500 mW cm^{-2}, respectively, and eventually flood at 100% RH. On the contrary, lung-inspired flow-field based PEMFCs with the implemented water management strategy showed 20% and 30% increase in maximum current and power density, respectively, with uninterrupted, flooding-free operation. This exceptional result implies that the employed water management strategy relies on capillary pressure to remove the water and not on gas flow, since this lung inspired flow-field demonstrates substantially less pressure drop than commercial serpentine flow-field based PEMFC (Fig. 5). Additional measurements are currently on-going to evaluate the performance of these flow-field based PEMFCs under different operating conditions.
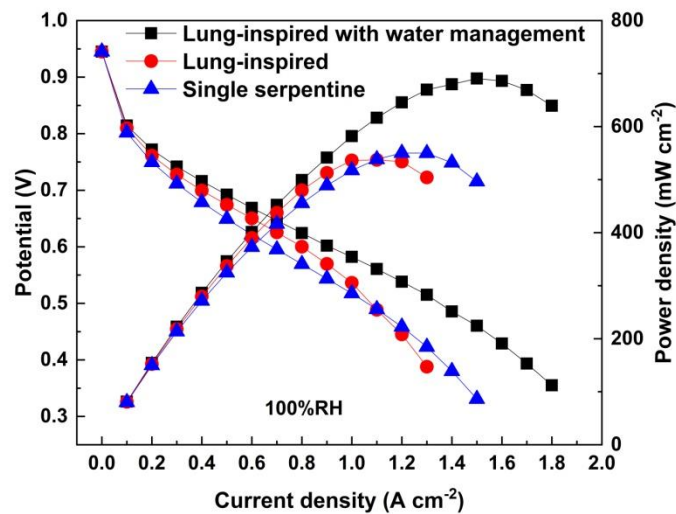

Figure 4. Polarization curves of lung-inspired ($N = 4$) with water management strategy implemented, lung-inspired ($N = 4$), and commercial, serpentine flow-field based PEMFCs at 100% RH (10 cm^2 flow-field area).
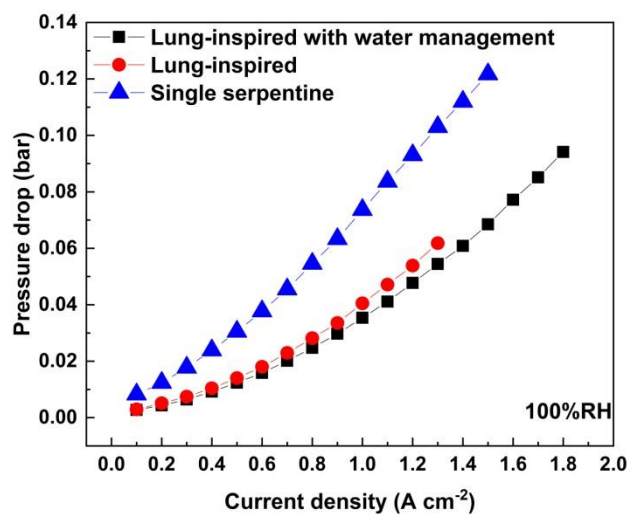

Figure 5. Pressure drop in the cathode for lung-inspired and serpentine flow-field (10 cm^2 surface area) based PEMFCs at 100% RH (10 cm^2 flow-field area).

Conclusions

A nature-inspired engineering methodology was employed to solve the flooding issue at high RH in PEMFCs. Inspiration was derived from the water drinking mechanism employed by certain lizards living in arid regions, which relies on capillary action.

This water management strategy differs from the one we reported earlier.(11) The water removal mechanism in our previous publication(11) relies on the pressure difference between the gas and liquid water channel, whereas, herein, capillary pressure is utilized to wick the generated water.

A thin graphite plate with laser engraved capillaries was installed in our best performing lung-inspired flow-field based PEMFCs with $N = 4$ generations and their performance at 100% RH is compared to commercial serpentine flow-field and lung-inspired flow-field based PEMFCs.

Neutron imaging measurements of the lung-inspired flow-field based PEMFC ($N = 4$) with water management implemented revealed that water accumulation occurred only on the anode side, while water was rapidly removed from the cathode. As a result, initial performance results at 100% RH demonstrated a flood-free operation compared to commercial serpentine and lung-inspired flow-field based PEMFCs and a significant increase in current and power density. Detailed discussion about the water management strategy employed, characteristics of the graphite plate modified with capillaries, as well as analytical characterization and performance results will be presented in an upcoming publication.

Acknowledgments

References

1. P. Trogadas, J. I. S. Cho, T. P. Neville, J. Marquis, B. Wu, D. J. L. Brett and M. O. Coppens, *Energy & Environmental Science*, **11**, 136 (2018).
2. M.-O. Coppens, *Current Opinion in Chemical Engineering*, **1**, 281 (2012).
3. P. Trogadas and M.-O. Coppens, *Chemical Society Reviews*, **49**, 3107 (2020).
4. P. Trogadas and M.-O. Coppens, in *Sustainable Nanoscale Engineering*, G. Szekely and A. Livingston Editors, p. 19, Elsevier (2020).
5. P. Trogadas, M. M. Nigra and M.-O. Coppens, *New Journal of Chemistry*, **40**, 4016 (2016).
6. P. Trogadas, V. Ramani, P. Strasser, T. F. Fuller and M.-O. Coppens, *Angewandte Chemie International Edition*, **55**, 122 (2016).
7. J. I. S. Cho, J. Marquis, P. Trogadas, T. P. Neville, D. J. L. Brett and M. O. Coppens, *Chemical Engineering Science*, **215**, 115375 (2020).

8. J. I. S. Cho, T. P. Neville, P. Trogadas, Q. Meyer, Y. Wu, R. Ziesche, P. Boillat, M. Cochet, V. Manzi-Orezzoli, P. Shearing, D. J. L. Brett and M. O. Coppens, *Energy*, **170**, 14 (2019).
9. P. Comanns, G. Buchberger, A. Buchsbaum, R. Baumgartner, A. Kogler, S. Bauer and W. Baumgartner, *Journal of The Royal Society Interface*, **12**, 20150415 (2015).
10. I. Manke, H. Markötter, T. Arlt, C. Tötzke, M. Klages, J. Haußmann, S. Enz, F. Wieder, J. Scholta, N. Kardjilov, A. Hilger and J. Banhart, *Physics Procedia*, **69**, 619 (2015).
11. J. I. S. Cho, T. P. Neville, P. Trogadas, J. Bailey, P. Shearing, D. J. L. Brett and M. O. Coppens, *International Journal of Hydrogen Energy*, **43**, 21949 (2018).